J Inorg Organomet Polym (2011) 21:412–420
DOI 10.1007/s10904-011-9483-9

Synthesis and Characterization of SiC(Ti) Ceramics Derived from a Hybrid Precursor of Titanium-Containing Polycarbosilane

Zhaoju Yu · Junying Zhan · Cong Zhou · Le Yang · Ran Li · Haiping Xia

Received: 20 November 2010 / Accepted: 17 March 2011 / Published online: 30 March 2011

Abstract A hybrid precursor of titanium-containing polycarbosilane is prepared by blending hyperbranched polycarbosilane (HBPCS) and tetrabutyl titanate (TBT), and then crosslinking at 160 °C, followed by pyrolyzing at high temperatures to afford SiC(Ti) ceramics. The crosslinking reaction of HBPCS–TBT hybrid precursor is investigated by FT-IR, solid state ^{29}Si MAS NMR, and GPC. The results indicate that the crosslinking reaction takes place via condensation between the Si–H bond of HBPCS and butoxy group in TBT leading to the formation of Si–O–Ti bonds. The thermal properties and structural evolution of crosslinked hybrid precursor and the crystallization behavior and composition of final ceramics are investigated by TGA, FT-IR, Raman spectroscopy, XRD and energy dispersive elemental analysis. The ceramic yield of hybrid precursor is significantly enhanced by introduction of TBT. The ceramic yield at 1,400 °C is 83% for HBPCS–TBT-5 as measured by TGA. The Ti-content in the ceramic is controlled by varying the TBT content in the feed. The SiC(Ti) ceramic is amorphous at 900 °C. The characteristic peaks of β-SiC and TiC appear until 1,600 °C. The growth of SiC crystals is inhibited by the formation of TiC.

Z. Yu (✉) · J. Zhan · C. Zhou · L. Yang · R. Li · H. Xia (✉)
College of Materials, Key Laboratory of High Performance Ceramic Fibers (Xiamen University), Ministry of Education, Xiamen 361005, China
e-mail: zhaojuyu@xmu.edu.cn

H. Xia
e-mail: hpxia@xmu.edu.cn

H. Xia
College of Chemistry & Chemical Engineering, Xiamen University, Xiamen 361005, China

Keywords Silicon carbide · Hyperbranched polycarbosilane · Tetrabutyl titanate · Hybrid precursor

1 Introduction

Polycarbosilanes (PCS) have been of particular interest as precursors to SiC, an important high temperature structural ceramic and semiconductor material [1]. Of all the PCS, liquid hyperbranched PCS (HBPCS) may be regarded as excellent effective precursors especially for a matrix source because of their unique structures and favorable properties [2, 3]. Whitmarsh and Interrante [4] reported the first HBPCS obtained by the Grignard reaction of $ClCH_2SiCl_3$ in ether, yielding a liquid hydridopolycarbosilane (HPCS) with an approximate compositional formula $[SiEtH_{1.85}CH_2]_n$. Thus, HPCS, due to its relatively high crosslinking temperature (ca. 300 °C) and loss of volatile oligomeric components, occurs upon unconfined pyrolysis in a flowing nitrogen atmosphere to give a ceramic yield of ca. 55% [2, 3].

Generally speaking, ceramic yield is an important factor to evaluate a polymer precursor. Many efforts have been devoted to increasing the ceramic yield of liquid HBPCS. Initially, unsaturated carbon–carbon bonds were introduced onto the HBPCS [5–7]. A commercial allyhydridopolycarbosilane (AHPCS) was explored via the introduction of allyl side groups onto the backbone of the HPCS. This material was widely studied for its excellent properties as a SiC precursor [5–7]. About 2.5–10% substitution of allyl groups has been found sufficient to increase the ceramic yield at 1,000 °C to 70–80%. It was reported that the enhancement of the ceramic yield of AHPCS and the lowering of the effective crosslinking temperature (to ca. 200 °C), is attributed to the

contribution of a thermally induced intramolecular hydrosilylation crosslinking reaction [2, 3]. It is well known that processing ceramic materials by polymer precursors involves the synthesis of the precursor followed by crosslinking into an unmeltable preceramic network and finally pyrolysis at elevated temperatures [8, 9]. Polymer crosslinking prior to pyrolysis, which is conventionally carried out by heating the polymer in the atmosphere, is required to increase the ceramic yield [10]. Recently, crosslinking reactions involving HBPCS were investigated to enhance the ceramic yield [11–13]. Our research, therefore, sought an efficient crosslinking agent to lower the crosslinking temperature and enhance the ceramic yield in HBPCS [14].

The incorporation of transition metals such as Fe, Co, Ni and Ti into ceramics is very attractive as it leads to materials with interesting catalytic, magnetic, electrical, and optical properties [15–23]. Among these metal-containing ceramics, SiC reinforced with TiC exhibits more enhanced properties of toughness, strength, and especially thermal-shock resistance than any of the component pure phases does [21–23]. This is because since TiC has excellent thermal stability, which can serve as intergranular phases of SiC. This prevents grain boundary migration under high temperatures and offsets the stringent thermal gradients imposed by aerothermal heating. It was reported that SiC–TiC fiber was synthesized by the reaction of tetrabutyl titanate (TBT) with Yajima PCS, which was prepared by the thermal decomposition of polydimethylsilane [24–27]. In the Yajima PCS/TBT system, the formation of a crosslinked structure by a condensation between Si–H bonds of PCS and TBT was reported [28].

It was reported that the HBPCS has more reactive Si–H bonds (e.g., SiH, SiH_2 and SiH_3) compared to the Yajima PCS [29–32]. In this work, we used TBT for the first time as a crosslinking agent to improve the crosslinking of HBPCS. A more detailed crosslinking mechanism of the HBPCS–TBT hybrid precursor was clarified, and an in situ synthesis of SiC reinforced with TiC; namely, SiC(Ti) ceramics by polymer pyrolysis was investigated.

2 Experimental

2.1 Materials

HBPCS with formula $[SiH_{1.55}(CH_3)_{0.45}CH_2]_n$ was prepared (previously described) by a one-pot synthesis with $Cl_2Si(CH_3)CH_2Cl$ and Cl_3SiCH_2Cl as the starting materials [29]. HBPCS used in this work has a number-average molecular weight of ca. 1,260 and a polydispersity index of 1.89. TBT (99% purity, Aldrich) was used as received. All manipulations were carried out in an inert gas atmosphere.

2.2 Crosslinking of HBPCS–TBT Hybrid Precursor

Crosslinking of the HBPCS–TBT hybrid precursor was carried out in a Schlenk flask with a magnetic stirrer and an argon inlet. A mixture of HBPCS and TBT was introduced into the Schlenk flask at room temperature under argon with stirring until a clear solution was obtained. The weight ratio of Ti to HBPCS was 1, 2, 3, and 5% and labeled correspondingly as HBPCS–TBT-1, HBPCS–TBT-2, HBPCS–TBT-3 and HBPCS–TBT-5. The Schlenk flask was then heated to 160 °C in an oil bath. During the heat treatment, the solution turned from pale orange to green and then to dark blue. The liquid HBPCS–TBT solution became a compact black rubbery solid after 24-h at this temperature. These solid samples were used both for TGA and for macroscopic pyrolysis.

2.3 Macroscopic Pyrolysis of HBPCS–TBT Hybrid Precursor

For Tp < 900 °C (Tp = highest pyrolysis temperature), the crosslinked sample was put in a graphite crucible and heated in a glass silica tube under an argon flow. The temperature was progressively raised to the Tp at a rate of 5 °C/min and kept at this value for 2-h. For Tp > 900 °C, the sample (pre-pyrolyzed at 900 °C) was put in a graphite crucible, heated rapidly to Tp at a rate of 40 °C/min and kept at this temperature for 2 h under an argon flow. After pyrolysis, the resulting ceramic was furnace-cooled to RT.

2.4 Characterization

FT-IR spectra (transmission mode) were obtained with a Nicolet Avator 360 apparatus (Nicolet, Madison, WI) on KBr plates for liquid samples and as KBr disks for solid samples. Gel permeation chromatography (GPC) was performed using an Agilent 1100 system (Agilent, Palo Alto, CA) at 35 °C in THF as the eluant (flow rate, 1.0 mL/min). Average molecular weights were obtained from narrow polystyrene standards. Solid-state ^{29}Si-magic angle spinning nuclear magnetic resonance (^{29}Si MAS NMR) experiments were performed on a Bruker AV 300 NMR spectrometer using a 4.0 mm Bruker double resonance MAS probe. The samples were spun at 5.0 kHz. The ^{29}Si isotropic chemical shifts were referenced to tetramethylsilane. Thermal analysis for the pyrolytic conversion of the cured CPSZ was performed by thermogravimetric analysis (TGA) (Netzsch STA 409C, Netzsch, Germany) in argon gas at a heating rate of 10 °C/min from room temperature to 1,400 °C. X-ray diffraction (XRD) studies were carried out with a PANalytical X'Pert PRO diffractometer (PANalytical, Netherlands) with Cu $K\alpha$ radiation ($\lambda = 1.54178$ Å). The specimens were continuously scanned from 10° to 90°

(2θ) at a speed of 0.0167°/s. Raman spectra were recorded on a Raman spectrometer (LabRam I, Dilor, France). Elemental analysis of ceramics was performed with an energy dispersive spectrometer (EDS, JEOL, Japan).

3 Results and Discussions

3.1 Cross-Linking

The cross-linking reaction of HBPCS–TBT hybrid precursor was investigated by FT-IR. The assignment of HBPCS was described elsewhere [30–32] as follows: 2140 cm^{-1} (vs, Si–H stretching), 940 cm^{-1} (vs, Si–H bending), 2950, 2873 cm^{-1} (s, CH_3 stretching), 2920 cm^{-1} (s, CH_2 stretching), 1400, 1250 cm^{-1} (Si—CH_3 deformation), 1355 cm^{-1} (s, Si—CH_2—Si deformation), 1040 cm^{-1} (vs, Si—CH_2—Si stretching), 800 cm^{-1} (vs, Si–C stretching). From a comparison of the FT-IR spectra of crosslinked HBPCS–TBT (Fig. 1c–f) with those of HBPCS and TBT (Fig. 1b and a), respectively, it is observed that crosslinked HBPCS–TBT consists of characteristic peaks of HBPCS and TBT.

As reported previously, the intensity ratio of the peaks at 2,140 cm^{-1} (Si–H) to 1,250 cm^{-1} (Si–CH_3) were denoted as A_{2140}/A_{1250}, and the value of A_{2140}/A_{1250} indicates the Si–H content [14]. The A_{2140}/A_{1250} value for the original HBPCS is 20.5, while those of HBPCS–TBT-1, HBPCS–TBT-2, HBPCS–TBT-3 and HBPCS–TBT-5 are 19, 18.9, 18.1 and 16.5, respectively. Obviously, the A_{2140}/A_{1250} value gradually decreases with the increase of Ti contents in feed, indicating that Si–H bonds are involved in the crosslinking. Moreover, it is worth mentioning that the C–H deformation in the CH_3 group of TBT at 1,460 cm^{-1} and Ti–O–C absorption peak at 1,090 cm^{-1} appear in the crosslinked HBPCS–TBT [33], which suggests that some $Ti(OCH_2CH_2CH_2CH_3)_4$ groups remained as pendant groups. As reported, Si–O–Ti was formed in the Yajima PCS/TBT system and its absorption appeared at 920 cm^{-1} [24], which might overlap with the Si–H bending at 940 cm^{-1}. However, the existence of Si–O–Ti bond is ambiguous using FT-IR.

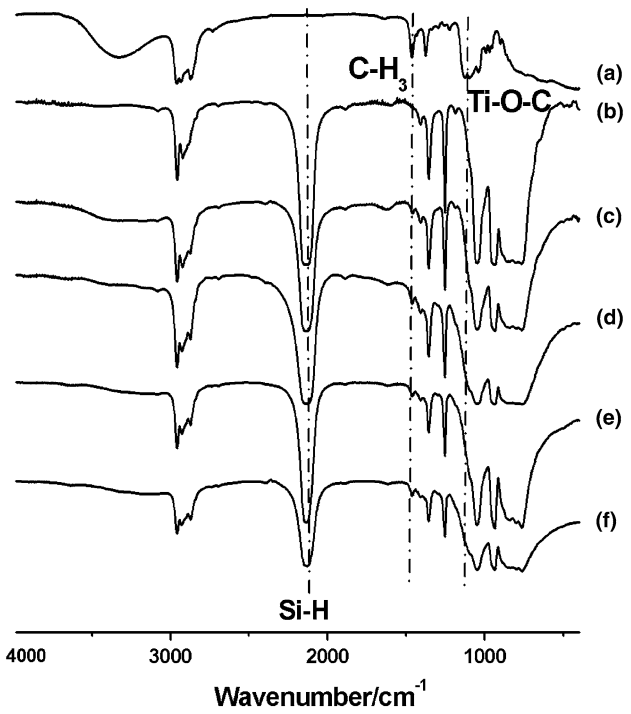

Fig. 1 FT-IR spectra of (*a*) TBT, (*b*) original HBPCS, and crosslinked (*c*) HBPCS–TBT-1, (*d*) HBPCS–TBT-2, (*e*) HBPCS–TBT-3 and (*f*) HBPCS–TBT-5 treated at 160 °C

With respect to the reaction mechanism, it was reported that the condensation of Si–H bonds between the Yajima PCS and the substituent group of TBT could occur. The reaction is a nucleophilic attack of a lone pair electrons of an O-atom to a Si-atom [28]. In the present study, HBPCS has more reactive Si–H bonds, such as SiH, SiH_2 and SiH_3, relative to the Yajima PCS [30–32]. We believe that the HBPCS–TBT crosslinking mechanism is similar to that for the Yajima PCS. Thus, the O-R_2 bond in TBT is cleaved and new Si–O–Ti bond is generated, which is accompanied by the release of butane (R_2H) (Fig. 2); namely, HBPCS is efficiently crosslinked by TBT. In this reaction mechanism, it is presumed that a Si–O–Ti bond is formed by reaction of Si–H in the PCS with the butoxy group in TBT. However, the existence of a Si–O–Ti characteristic absorption band is not confirmed by FT-IR.

However, as the HBPCS–TBT hybrid precursors become insoluble upon curing at intermediate temperatures, solid-state NMR may be applied to investigate the chemical structural changes. The solid-state ^{29}Si MAS NMR spectrum of crosslinked HBPCS–TBT and ^{29}Si NMR spectrum in solution of the original HBPCS are shown in Fig. 3. As reported previously, complex multiplets centered at 5 ppm (tetraalkyl silicon, SiC_4), from −10 to −20 ppm (monohydridosilicon, C_3SiH), from −30 to −40 ppm (dihydridosilicon, C_2SiH_2) and from −55 to −60 ppm (trihydridosilicon, $CSiH_3$) support a branched structure [4, 30–32]. For the ^{29}Si MAS NMR spectrum of HBPCS–TBT-5, the intensity of $CSiH_3$ (−55 to −65 ppm) end-groups significantly decreases while those of SiC_4, C_3SiH and C_2SiH_2 change little. The results indicate that $CSiH_3$ is more reactive than C_3SiH and C_2SiH_2, which is consistent with our previous work [34]. It is worth mentioning that a new peak centered at 15 ppm appears. This peak, which has been previously reported, may be due to the Si–O–Ti unit [33]. The fact that the intensity of $CSiH_3$ groups significantly decreases and Si–O–Ti units appear

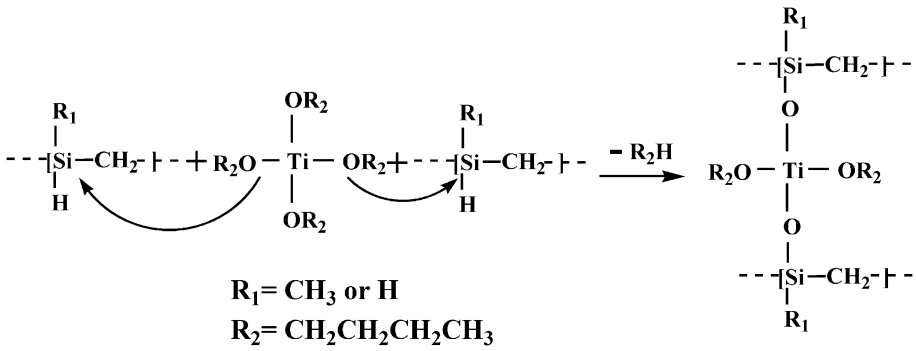

Fig. 2 Cross-linking mechanism of HBPCS–TBT hybrid precursors

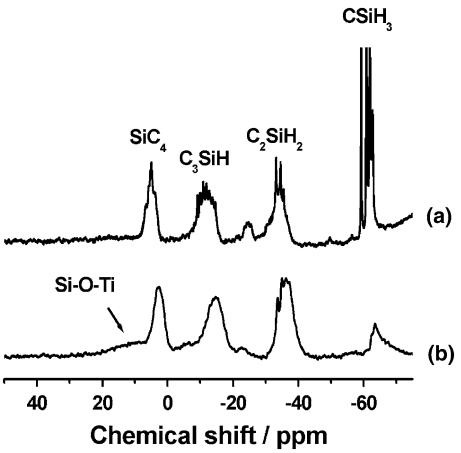

Fig. 3 ^{29}Si NMR spectrum of (*a*) the soluble original HBPCS in $CDCl_3$ and (*b*) solid-state ^{29}Si MAS NMR spectrum of HBPCS–TBT-5 treated at 160 °C for 24 h

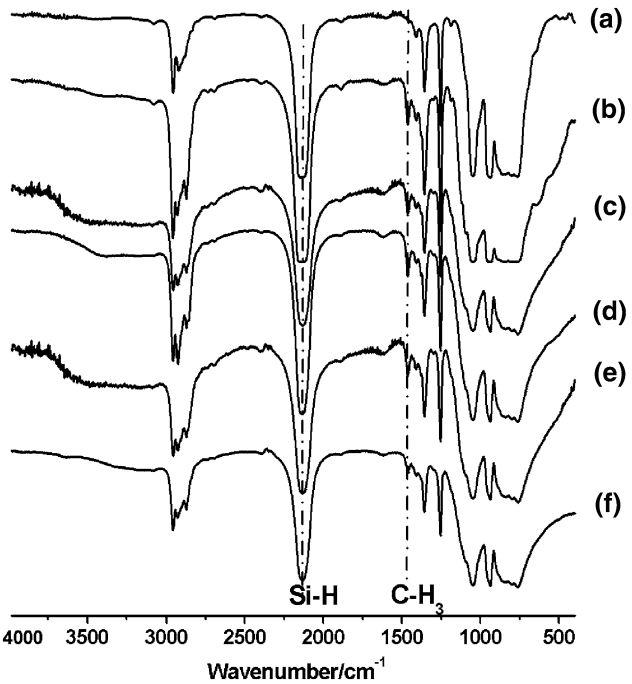

Fig. 4 FT-IR spectra of (*a*) original HBPCS, (*b*) HBPCS–TBT-5 mixture and cross-linked HBPCS–TBT-5 treated at 160 °C for (*c*) 1 h, (*d*) 2 h, (*e*) 4 h, and (*f*) 24 h

strongly supports a crosslinking mechanism of the HBPCS–TBT hybrid precursors.

To understand further the structural evolution of the hybrid precursors during the crosslinking reaction, HBPCS–TBT-5 samples prepared with different reaction times were examined by FT-IR (Fig. 4). Thus, the peak at 2,140 cm^{-1}, assigned to Si–H, and the peak at 1,460 cm^{-1}, due to CH_3 deformation of TBT, significantly weakens as the crosslinking time increases. This strongly supports crosslinking via condensation between Si–H bonds in HBPCS and butoxy group in TBT.

According to the crosslinking reaction (Fig. 2), the molecular weight of the hybrid precursor should increase. Subsequently, samples including the original HBPCS, the HBPCS–TBT-5 mixture and the crosslinked HBPCS–TBT-5 were subjected to GPC analysis (Fig. 5). The HBPCS and HBPCS–TBT-5 mixture show a similar GPC trace. When HBPCS–TBT-5 is heated at 160 °C for only 1 h, the GPC shows some high-molecular-weight peaks. A high-molecular-weight peak at about 100,000 Da is detected and is observed at a crosslinking time of 2 h. The sample heated for 4 h is insoluble in organic solvents, which precludes GPC analysis. The GPC results thus indicate that crosslinking leads to increasing molecular weight, as expected.

3.2 Ceramization

To understand the thermal behavior during pyrolytic conversion of the HBPCS–TBT hybrid precursor, the TGA was examined (Fig. 6). Generally, the mass of the residue is constant at temperatures above 900 °C indicating that the organic groups in HBPCS and HBPCS–TBT-5 decompose below this temperature. From 900 to 1,400 °C under nitrogen, a negligible mass change occurs indicating excellent heat-resistance. At 1,400 °C the ceramic yield is 83% for HBPCS–TBT-5 and 65% for HBPCS. Thus, the ceramic yield is significantly enhanced by introduction of

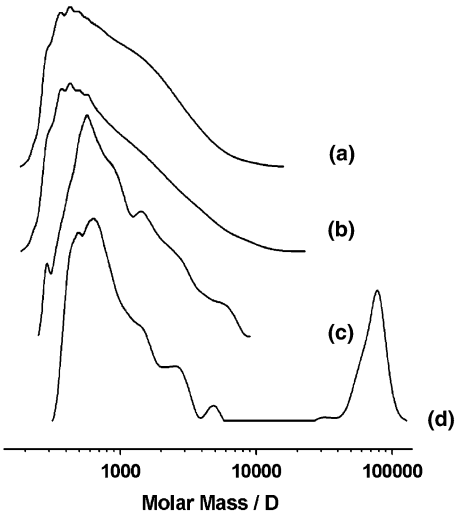

Fig. 5 GPC traces of (*a*) original HBPCS, (*b*) HBPCS–TBT-5 mixture, and cross-linked HBPCS–TBT-5 treated at 160 °C for (*c*) 1 h and (*d*) 2 h

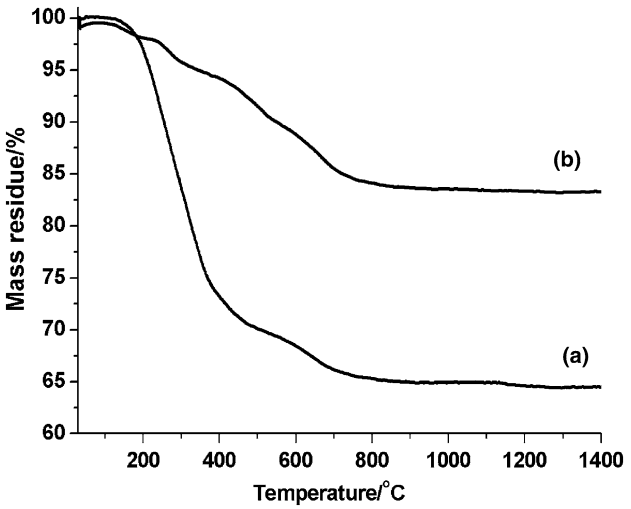

Fig. 6 TGA curves of (*a*) original HBPCS and (*b*) HBPCS–TBT-5 treated at 160 °C for 24 h

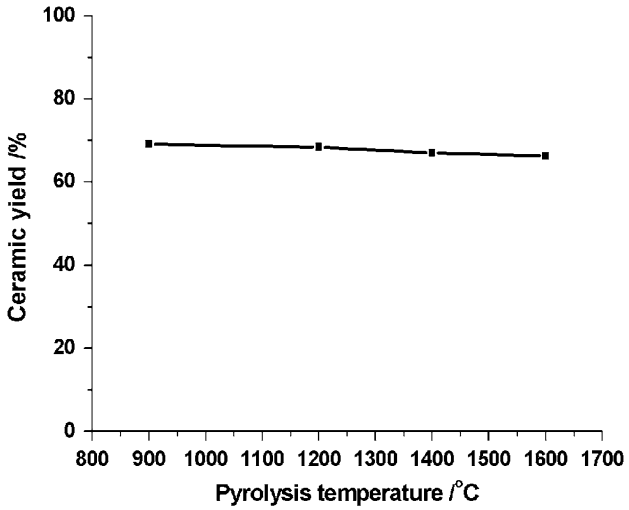

Fig. 7 Dependence of ceramic yields of HBPCS–TBT-5 on pyrolysis temperatures

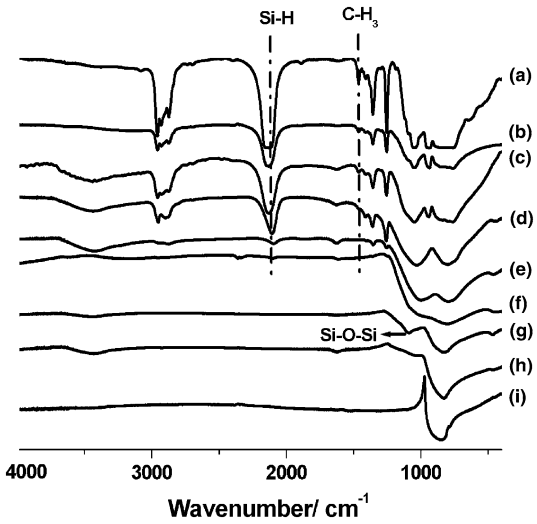

Fig. 8 FT-IR spectra of (*a*) HBPCS–TBT-5 mixture and cross-linked HBPCS–TBT-5 treated at (*b*) 160 °C, (*c*) 300 °C, (*d*) 500 °C, (*e*) 700 °C, (*f*) 900 °C, (*g*) 1200 °C, (*h*) 1400 °C, and (*i*) 1600 °C

TBT. At 400 °C, HBPCS shows a weight loss of 27% whereas HBPCS–TBT-5 has a weight loss of 6%. From 400 to 900 °C, HBPCS and HBPCS–TBT-5 have a weight loss of 8 and 10%, respectively. It seems that the significant difference between HBPCS and HBPCS–TBT-5 is the weight loss occurring below 400 °C. It has been reported that the weight loss of PCS below 400 °C is predominately oligomer evaporation [35]. The results here suggest that oligomers are efficiently crosslinked by TBT, which markedly reduces oligomer evaporation. Hence, a higher ceramic yield is obtained for the HBPCS–TBT hybrid precursor.

The TGA of crosslinked HBPCS–TBT gives a ceramic yield of 83% at 1,400 °C. However, the macroscopic pyrolysis experiment gives a lower yield, ~70% (Fig. 7), presumably because of the lower heating rate and the different heat history. In the latter case, the ceramic yield varies little from 900 to 1,600 °C, which is consistent with the TGA results.

The structural evolution of the polymer-to-ceramic conversion was investigated by FT-IR (Fig. 8). The absorption of CH_3 in TBT and SiH in HBPCS markedly decreases after heat treatment at 160 °C relative to the room temperature experiment This suggests that cross-linking of Si–H with TBT occurs at 160 °C and is accompanied by the cleavage of O–C bond in TBT. As a result, the CH_3 peak intensity (FT-IR) in the Ti–$OCH_2CH_2CH_2CH_3$ unit decreases. The FT-IR spectra at

300 °C is similar to that at 160 °C. The absorption of CH_3 in TBT and SiH in HBPCS decreases due to further crosslinking of SiH with TBT. At 500 °C, the characteristic CH_3 peak at 1,460 cm^{-1} almost vanishes, indicating that crosslinking is complete. The intensity of Si–H at 2,140 cm^{-1} decreases markedly and the Si–H bending mode at 940 cm^{-1} almost vanishes. It is believed that at 500 °C dehydrocoupling crosslinking (i.e., reaction of Si–H with Si–H), where the rate becomes significant only above ~300 °C [35], may be responsible for the decrease in Si–H intensity. Moreover, the Si–O–Ti absorption at 920 cm^{-1} overlaps with the Si–H bending mode, which almost disappears. Thus, the decomposition of Si–O–Ti is probably complete at 500 °C. Hasegawa [25] reported that the Si–O–Ti bond decomposes gradually above 200 °C and almost disappears at 400 °C. The Si–O–Ti decomposition leads to the formation of Si–O–Si bond [24].

In the present study, the intensity of broad peak centered at 1,040 cm^{-1} increases, indicating the formation of Si–O–Si bond (1,100–1,000 cm^{-1}). Therefore, the oxygen bonded to titanium is removed as a siloxane bond, leading to the formation of TiC [24, 25]. At 700 °C, the Si–H peak at 2,100 cm^{-1} disappears due to further dehydrocoupling crosslinking. Also, the absorption of Si–CH_3 at 1,250 cm^{-1} significantly reduces, which is attributed to the decomposition of organic side groups [36]. The Si–CH_2–Si bond gradually decomposes at 900 °C to form SiC, as confirmed by the decrease in the band at 1,040 cm^{-1} (Si–CH_2–Si); only one broad peak is retained at ~780 cm^{-1}, which is attributed to the amorphous SiC framework structure [35].

Upon further heating to 1,200 °C, the broad peak at ~780 cm^{-1} splits into two peaks; i.e., an Si–O–Si absorption at 1,090 cm^{-1} and an SiC absorption at 800 cm^{-1}. At 1,400 °C, the intensity of Si–O–Si absorption decreases rapidly and is accompanied by an increase in the crystallized SiC absorption at 820 cm^{-1}. The latter might be a result of the formation of crystallized SiC from the Si–O bond and free carbon at high temperature [24]. Further heating to 1,600 °C leads to a sharpening of the SiC band and a shift in its position from 780 to 840 cm^{-1}, which is consistent with the formation of crystalline SiC [37].

To analyze the ceramic composition, the EDS elemental analysis of the 1,600 °C ceramics was examined. The result is shown in Fig. 9. The EDS spectrum exhibits characteristic peaks of silicon, titanium and carbon thereby confirming the ceramic elemental composition.

The chemical composition of the SiC(Ti) ceramics, as locally assessed by EDS, is presented in Fig. 10. For HBPCS–TBT-1, 2, 3, and 5, the Ti weight percents in the hybrid precursor are 0.9, 1.8, 2.5, and 3.7% and those in ceramics are 2, 4.1, 5.8, and 8.4%, respectively. It is worth mentioning that the ceramic yield increases linearly with an increase in the Ti content of the precursor. Moreover, the

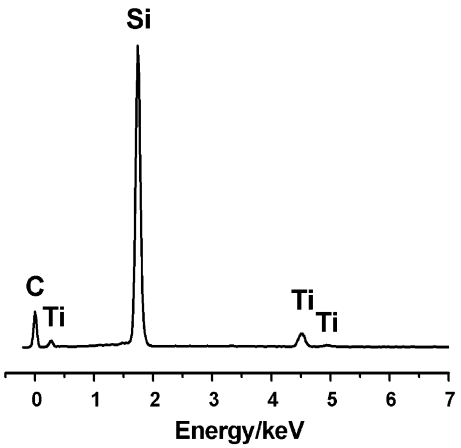

Fig. 9 EDS elemental analysis of 1,600 °C ceramics derived from HBPCS–TBT-5

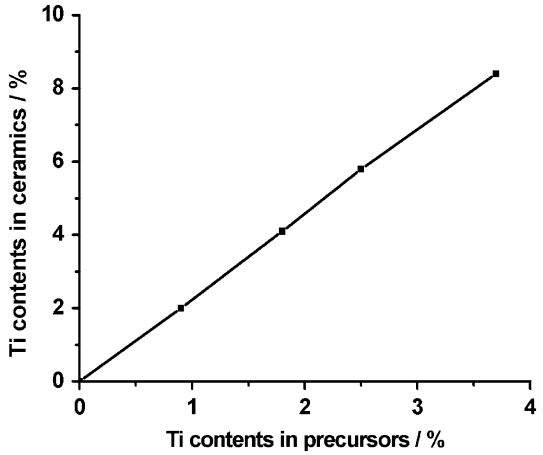

Fig. 10 Dependence of Ti content in 1,600 °C ceramics on Ti feed

Ti content in the ceramics can be controlled by varying the Ti content in feed.

3.3 Crystallization

The evolution of the crystalline phases was studied by XRD. The results (Fig. 11) show that the 900 °C ceramic is amorphous and highly disordered, which agrees well the FT-IR data. Further heating at 1,200 °C leads to the formation of graphite and incomplete crystallization. At 1,400 °C, the intensity of broad peak at 36° increases, which indicates SiC or TiC is more ordered relative to the material obtained at 1,200 °C. However, the assignments of diffraction peaks are ambiguous because the diffraction lines of β-SiC phase and TiC phase are very similar. The diffraction peak of graphite almost disappears indicating that the content of free carbon is reduced at 1,400 °C. This too agrees with the FT-IR, which supports the formation of

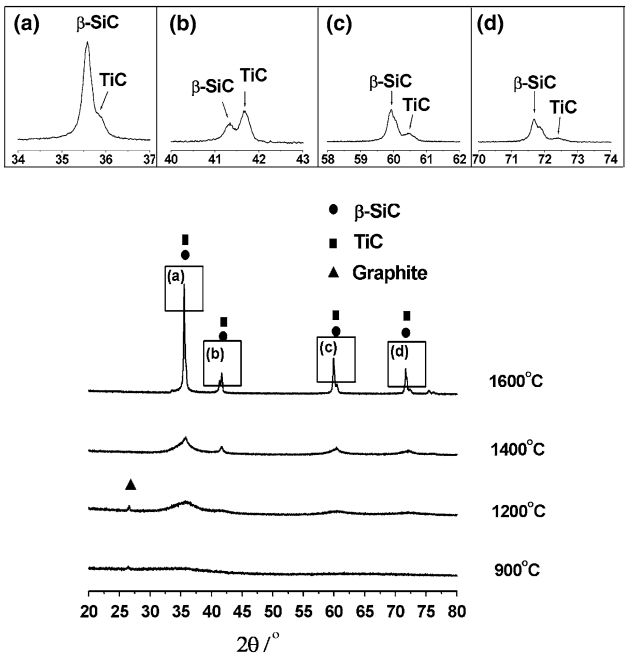

Fig. 11 XRD patterns of HBPCS–TBT-5 derived ceramics pyrolyzed at different temperatures

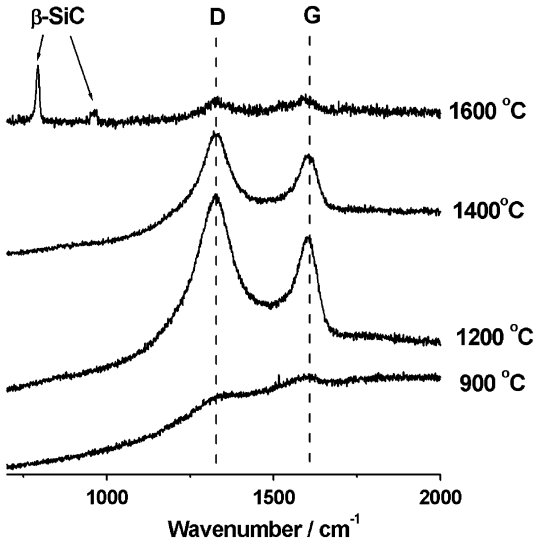

Fig. 12 Raman spectra of HBPCS–TBT-5 derived ceramics pyrolyzed at different temperatures

crystallized SiC from the Si–O bond and free carbon at 1,400 °C. The characteristic peaks of β-SiC and TiC appear at 1,600 °C; and, the TiC diffraction peak can be distinguished from that of β-SiC. Among these peaks, the three major peaks at $2\theta = 35.6°$ (111), 60.1° (220), and 71.8° (311) along with the weaker peak at 41.3° (200) are attributed to β-SiC. The peaks at $2\theta = 35.8°$ (111), 41.4° (200), 60.3° (220), and 72.1° (113) are due to the characteristic diffraction peak of TiC and is consentient with published data [38]. These XRD patterns also indicate that the heat treatment significantly influences the evolution of crystalline β-SiC and TiC.

Raman spectroscopy is a sensitive method for the characterization of carbon modifications. Raman investigations were carried out to get insight into the correlation between the evolution of free carbon and the crystallization of SiC (Fig. 12). In the Raman spectrum of the 900 °C ceramic, no signals are observed. At 1,200 °C, two peaks centered around 1,330 and 1,600 cm^{-1} are discernable, which correspond to the D and G peaks observed in free carbon [39]. The Raman spectrum indicates that the carbon network interconnects at long distances to form free carbon at 1,200 °C. At 1,400 °C, the intensity of the free carbon peaks significantly decreases. At 1,600 °C, two new bands centered at 790 and 960 cm^{-1}, attributed to β-SiC appear, are accompanied by a rapid decrease of the free carbon absorption band, which is consistent with the FT-IR and XRD analysis. The decrease may be due to the reaction of free carbon with Si–O to form crystallized SiC.

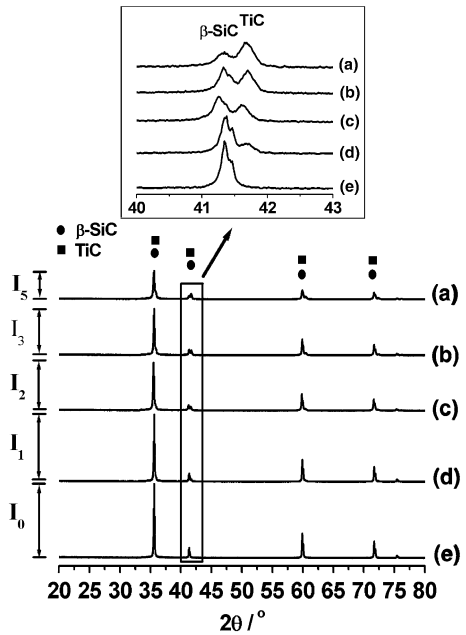

Fig. 13 XRD patterns of 1,600 °C ceramics derived from (*a*) HBPCS–TBT-5, (*b*) HBPCS–TBT-3, (*c*) HBPCS–TBT-2, (*d*) HBPCS–TBT-1, and (*e*) HBPCS

The effect of TBT content on the 1,600 °C ceramics was investigated (Fig. 13). The peak at 41.4° (200) of TiC, which is always the preferential orientation of grain growth, may be distinguished from the (200) peak of SiC. Furthermore, the intensity of the TiC peaks increases with feeding of TBT. In the HBPCS–TBT-5 pattern, the TiC (002) peak became more intense than the SiC (200) peak. The intensity of the SiC (111) peaks in HBPCS-derived ceramic is assigned as I_0. Similarly, those of HBPCS–TBT-1, HBPCS–TBT-2,

HBPCS–TBT-3, and HBPCS–TBT-5-derived ceramics are assigned I_1, I_2, I_3, and I_5, correspondingly. The order of intensities is followed as: $I_0 > I_1 > I_2 > I_3 > I_5$. From the TGA experiments, for HBPCS–TBT-1, 2, 3, and 5, the Ti weight percents in 1,600 °C ceramics are 2, 4.1, 5.8, and 8.4%, respectively. With the increase in Ti contents of ceramics, the intensity of the β-SiC (111) peak is significantly reduced indicating that the growth of SiC crystals is inhibited by the formation of TiC.

4 Conclusions

The synthesis of SiC(Ti) ceramics derived from a hybrid precursor of titanium-containing polycarbosilane was demonstrated and involves the blending of HBPCS and TBT and cross-linking at 160 °C. This is followed by the pyrolysis at high temperatures. The crosslinking reaction of HBPCS–TBT hybrid precursor was investigated by FT-IR, solid state ^{29}Si MAS NMR, and GPC. The results indicate that crosslinking takes place via condensation of the Si–H bonds in HBPCS and the Ti-$OCH_2CH_2CH_2CH_3$ bonds of TBT to give Si–O–Ti. The ceramization process of HBPCS–TBT hybrid precursor was studied by TGA and FT-IR. The TGA results indicate that the ceramic yield of hybrid precursor is significantly enhanced by introduction of TBT, which may be due to the fact that crosslinking between HBPCS and TBT markedly reduces the evaporation of low-molecular-weight oligomers. The FT-IR results suggest that during the heat treatments the hybrid precursor undergoes crosslinking, an organic-to-inorganic transition and a conversion of amorphous to crystalline SiC(Ti). The composition of the 1,600 °C ceramics was measured by EDS elemental analysis and indicated that the Ti content in the ceramics could be readily controlled by varying the TBT content in the feed. Finally, the crystallization behavior of the hybrid precursor-derived ceramics was characterized by XRD. The data demonstrate that SiC(Ti) ceramic is amorphous at 900 °C and the characteristic peaks of β-SiC and TiC do not appear until 1,600 °C. The growth of SiC crystals is inhibited by the formation of TiC.

Acknowledgments The project was supported by National Natural Science Foundation of China (50802079), Aviation Science Foundation of China (2008ZH68005), and Natural Science Foundation of Fujian Province of China (Nos. 2008J0165 and 2010J01307).

References

1. K. Kita, M. Narisawa, A. Nakahira, H. Mabuchi, M. Itoh, M. Sugimoto, M. Yoshikawa, J. Mater. Sci. **45**, 139 (2010)
2. L.V. Interrante, Q.H. Shen, in *Silicon Containing Polymers*, ed. by R.G. Jones, et al. (Kluwer Academic Publishers, Dordrecht, 2000)
3. L.V. Interrante, Q.H. Shen, in *Silicon-Containing Dendritic Polymers*, vol. 2, ed. by P.R. Dvornic, M.J. Owen (Springer Science + Business Media B.V., Dordrecht, 2009), p. 315
4. C.K. Whitmarsh, L.V. Interrante, Organometallics **10**, 1336 (1991)
5. L.V. Interrante, K. Moraes, L. MacDonald, W. Sherwood, Ceram. Trans. **144**, 125 (2002)
6. M. Kotani, Y. Kato, A. Kohyama, M. Narisawa, J. Ceram. Soc. Jpn. **111**, 300 (2003)
7. J. Zheng, M. Akinc, J. Am. Ceram. Soc. **84**, 2479 (2001)
8. G. Ziegler, H.J. Kleebe, G. Molz, H. Müller, S. Traßl, W. Weibelzahl, Mater. Chem. Phys. **61**, 55 (1999)
9. N. Janakiraman, F. Aldinger, J. Eur. Ceram. Soc. **29**, 163 (2009)
10. P.E. Froehling, J. Inorg. Organomet. Polym. **3**, 251 (1993)
11. B.E. Fry, A. Guo, D.C. Nechers, J. Organomet. Chem. **538**, 151 (1997)
12. H.B. Li, L.T. Zhang, L.F. Cheng, Z.J. Yu, M.H. Huang, H.B. Tu, H.P. Xia, J. Mater. Sci. **44**, 721 (2009)
13. H.B. Li, L.T. Zhang, L.F. Cheng, H.T. Kang, Y.G. Wang, J. Mater. Sci. **44**, 970 (2009)
14. Z.J. Yu, J.Y. Zhan, M.H. Huang, R. Li, C. Zhou, G.M. He, H.P. Xia, J. Mater. Sci. **45**, 6151 (2010)
15. E.J. Houser, T.M. Keller, Macromolecules **31**, 4038 (1998)
16. A. Berenbaum, M. Ginzburg-Margau, N. Coombs, A.J. Lough, A. Safa-Sefat, J.E. Greedan, G.A. Ozin, I. Manners, Adv. Mater. **15**, 51 (2003)
17. J.Q. Lu, T.E. Kopley, N. Moll, D. Roitman, D. Chamberlin, Q. Fu, J. Liu, T.P. Russell, D.A. Rider, I. Manners, M.A. Winnik, Chem. Mater. **17**, 2227 (2005)
18. M. Ginzburg, J. MacLachlan, S.M. Yang, N. Coombs, T.W. Coyle, N.P. Raju, J.E. Greedan, R.H. Herber, G.A. Ozin, I. Manners, J. Am. Chem. Soc. **124**, 2625 (2002)
19. Q.H. Sun, K.T. Xu, H. Peng, R.H. Zheng, M. Haussler, B.Z. Tang, Macromolecules **36**, 2309 (2003)
20. L. Friebe, K. Liu, B. Obermeier, S. Petrov, P. Dube, I. Manners, Chem. Mater. **19**, 2630 (2007)
21. K.S. Cho, Y.W. Kim, H.J. Choi, J.G. Lee, J. Am. Ceram. Soc. **79**, 1711 (1996)
22. G. Wen, S.B. Li, B.S. Zhang, Z.X. Guo, Acta Mater. **49**, 1463 (2001)
23. L. Contreras, X. Turrillas, G.B.M. Vaughan, Å. Kvick, M.A. Rodríguez, Acta Mater. **52**, 4783 (2004)
24. Y.C. Song, Y. Hasegawa, S.J. Yang, M. Sato, J. Mater. Sci. **23**, 1911 (1988)
25. Y. Hasegawa, C.X. Feng, Y.C. Song, Z.L. Tan, J. Mater. Sci. **26**, 3657 (1991)
26. Y.C. Song, C.X. Feng, Z.L. Tan, Y. Lu, J. Mater. Sci. Lett. **9**, 1310 (1990)
27. G. Chollon, B. Aldacourrou, L. Capes, R. Pailler, R. Naslain, J. Mater. Sci. **33**, 901 (1998)
28. T. Ishikawa, T. Yamamura, K. Okamura, J. Mater. Sci. **27**, 6627 (1992)
29. Z.J. Yu, T.H. Huang, M.H. Huang, H.P. Xia, L.F. Chen, Y. Zhang, L.T. Zhang, J. Xiamen Univ. (Chin.) **47**, 692 (2008)
30. T.H. Huang, Z.J. Yu, X.M. He, M.H. Huang, L.F. Chen, H.P. Xia, L.T. Zhang, Chin. Chem. Lett. **18**, 754 (2007)
31. M.H. Huang, Y.H. Fang, R. Li, Z.J. Yu, H.P. Xia, L.F. Chen, J. Appl. Polym. Sci. **113**, 1611 (2009)
32. Y.H. Fang, M.H. Huang, Z.J. Yu, H.P. Xia, L.F. Chen, Y. Zhang, L.T. Zhang, J. Am. Ceram. Soc. **91**, 3298 (2008)
33. Y.X. Yu, Y.D. Guo, X. Cheng, Y. Zhang, J. Mater. Chem. **19**, 5637 (2009)
34. Z.J. Yu, Y.H. Fang, M.H. Huang, R. Li, J.Y. Zhan, C. Zhou, G.M. He, H.P. Xia, Polym. Adv. Technol. (2010). doi:10.1002/pat.1777
35. Q. Liu, H.J. Wu, R. Lewis, G.E. Maciel, L.V. Interrante, Chem. Mater. **11**, 2038 (1999)

36. E. Bouillon, F. Langlais, R. Pailler, R. Naslain, F. Cruege, P.V. Huong, J.C. Sarthou, J. Mater. Sci. **26**, 1333 (1991)
37. G. Ramis, P. Quintard, M. Gauchetier, G. Busca, V. Lorenzelli, J. Am. Ceram. Soc. **72**, 1692 (1989)
38. S. Yajima, T. Iwai, T. Yamamura, K. Okamura, Y. Hasegawa, J. Mater. Sci. **16**, 1349 (1981)
39. S. Trassl, G. Motz, E. Rossler, G. Ziegler, J. Am. Ceram. Soc. **85**, 239 (2002)